# Investigations of roughness-generated TBL sound using coupled physical-computational experiments in conjunction with theoretical development

W. Blake[a], K.-H. Kim[b], M. Goody[a], M. Wang[c], W. J. Devenport[d] and S. A L Glegg[e]

[a]Naval Surface Warfare Center (Ret.), 6905 Hillmead Road, Bethesda, MD 20817, USA
[b]Office of Naval Research, Randolph St., Arlington, VA 22202, USA
[c]University of Notre Dame, Departmernt of Aerospace and Mechanical Engineering, Notre Dame, MD 46556, USA
[d]Virginia Tech, Aerospace and Ocean Engineering, 224E Randolph Hall, Blacksburg, VA 24061, USA
[e]Florida Atlantic University, Department of Ocean Engineering, Boca Raton, VA 33431, USA
hydroacoustics@aol.com

Sound produced by turbulent-boundary layers (TBL) over rough walls is being studied in a series of physical-computational experiments. At issue is the development of an understanding of how the wall elements generate flow dipoles which directly determines how the sound is described in terms of dependent variables. The considered mechanisms include dipoles at the roughness elements due to their shed wakes, distributed surface dipoles due to convecting turbulence impinging onto elements, and Rayleigh-like scattering into sound of aerodynamic pressures of hydrodynamic wave numbers of flow above the roughness. The LES of rough-wall TBL consists of "numerical" experiments being used to isolate the separate mechanisms. These simulations are benchmarked with analysis and with matching physical experiments on rough wall patches in which identical geometries of wall roughness and identical Reynolds numbers are used. In the physical measurements, array-based measurements of the radiated sound are being used to characterize the directivity and magnitude of the sound and to relate the sound to aerodynamic wall pressure and to classical characteristics of the turbulent boundary layer. The LES produces for comparison both radiated sound and detailed flow structure around the roughness elements.

# 1    Introduction

Sound generated by turbulent boundary layer (TBL) flow over rough walls has been of continuing, yet intermittent, interest for nearly 40 years and a large body of work has been presented and published over that time. In spite of this there is still no coherent view of the physics of sound generation by rough-wall turbulent boundary layers. Space does not permit a comprehensive view of the literature extant on this subject area and so only a few references shall be cited here. Blake [1] has reviewed the body of work through 1986; the first relevant experimental work on the problem of *acoustic radiation* was conducted by Hersh [2]. In that work a small roughness patch was installed at the exit of a nozzle flow to provide the first controlled evaluation of sound emitted. The results cannot be usefully generalized to a broader context of engineering application, but they did give the initial view of dependence on speed and roughness. Then in the 1983-1991 time period Farabee and Geib [3] conducted a well-controlled measurement of sound radiated along the surface of a rigid wall downstream of a large patch of roughness. They obtained measurements of sound emitted downstream of the patch and along the wall for a variety of roughness configurations. Unfortunately the properties of the turbulent boundary layer were not comprehensively documented over the entire development of the flow. At the same time Howe [4] presented a theory in which sound is produced by inviscid scattering of turbulent boundary layer pressure generated by the boundary layer flow above, but not flowing around the roughness. In this way subsonic hydrodynamic wavenumbers are scattered into sound by the Rayleigh-like scattering at the elements beneath the boundary layer. The mechanism did not consider the sound that might be produced by the unsteady drag that is reaction at the wall due to the production of turbulence.

This paper is a short summary of the results currently in hand of a special-focus program to understand to quantify the sound produced by rough-wall turbulent boundary layers. Other papers at this meeting go into further depth. The current research program includes 2 new wind tunnel investigations [5,6], two analytical investigations [6,7,8] and a series of Large Eddy Simulations (LES) [9] which are tailored to understanding the mechanisms of sound generation by rough-wall turbulent boundary layers through a series of physical-numerical experiments that are mutually tailored. The concept used in developing these experiments is to link numerical and physical exercises into a common experiment in which the geometry, Reynolds number, and dependent and independent variables are common. This requires that the physical and numerical experiments are specified along the common requirements of that which is possible in the physical wind tunnel facility (speed, geometry, size) and that which is possible in the numerical modelling (gridding, boundary conditions, numerical capacity). Thus the exercises are designed along a series of compromises which are determined jointly by the physical experimenter and the numerical analyst. A subset of results of these will be outlined in the body of this paper.

# 2    Physics overview and experimental configurations

The sound from rough-wall turbulent boundary layers is considered due to three physical processes that are depicted in Fig. 1. First, at the top of the figure, interstitial flow in the immediate vicinity of a roughness element includes a "gust" response due to the incident turbulence that originates from upstream and is highly rotational. The interstitial flow is then fed by a viscous wake that is shed from the element; the upstream "gust" influences the wake production in ways that will be made clear in the LES. Moving on to the next roughness element, this flow becomes the "gust" inflow to it. The second contribution of sound generation is the inviscid scattering of aerodynamic pressure into sound by the roughness elements in the wall. In this mechanism the incident pressures are generated by the flow that grazes the tops of the roughness and lies above them. Notionally, the source of these pressure disturbances is the overall turbulent boundary layer as determined by the mean upstream shear. This incident pressure is characterized by subsonic convection wave number, $\omega/U_c(y_2)$, where $\omega$ is radian frequency and $U_c$ is local mean convection velocity at position $y_2$ above the wall. Both the first and second controlling mechanisms generate forces at the roughness elements, these forces constitute dipole sources at the wall. The third mechanism that is involved with the generation of sound is the reflection of the roughness dipoles due to the presence of the surface. If the flow were inviscid then it is well known that the reflection of normal stresses generates only quadrupole sound; the addition of fluctuating wall shear, either by the introduction of viscous wall stresses in the case of the smooth wall, or by the generation of stresses by either of the above two mechanisms, generates tangential dipole stresses which, under, reflection by the bounding rigid wall, become longitudinal quadrupoles of essentially the same radiation efficiency as the constituent dipole, itself.

Previous theoretical modelling of Howe [4] addresses this source. The theoretical modelling of Glegg, appearing in [6,11] addresses the generation of elemental dipole forces by convected vorticity and wake production; Martinez [7,8] further addresses the effect of local shear fluctuation and unsteady convection on the interstitial flow acoustics.

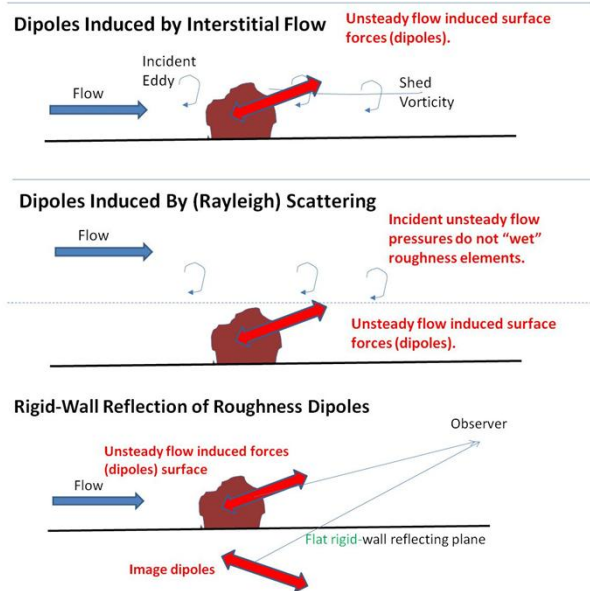The experimental program of physical measurement coupled with the LES is devoted to clarifying these mechanisms and to quantifying their relevance. The LES



Fig. 1 Illustration of flow-acoustic features of rough-wall flow .

experiments [9] will be conducted for patches of hemispherical roughness elements with a finite streamwise fetch that is entirely confined to a control volume as shown. The distribution of the roughness elements in this patch will evolve in stages from the single-element building block. The computation adds a second element in the wake of the first, then others to construct a total distribution of 40 elements. The LES will provide the details of flow among the interstices, the mean properties of the TBL as it
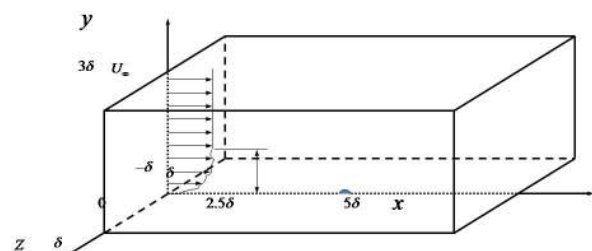


Fig. 2 Illustration of the LES control volume shown here enclosing the single-element building block of a distributed roughness. The volume occupies $5\delta x 2\delta x 3\delta$ with a smooth-wall inflow TBL which has momentum thickness Reynolds number of 7500, roughness element size is $h^+=95$.

develops over the fetch, and the sound radiated. Roughness sizes of $h^+=95$ and ~190 will be examined for comparison with wind-tunnel results from identical physical patches. The control volume and roughness used in the LES was

determined on the basis of a series of preliminary physical experiments that disclosed the attainable signal to noise for one of the rough-wall TBLs. The parallel physical experiment will exactly replicate the LES Reynolds number, roughness configuration and roughness fetch size. It will also mirror several of the computational iterations in terms of included numbers of roughness elements. This physical arrangement will be part of a larger series of
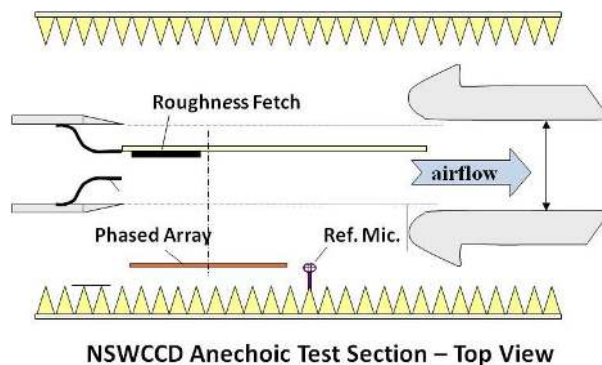


Fig. 3 Illustration of experimental arrangement of the NSWCCD group.
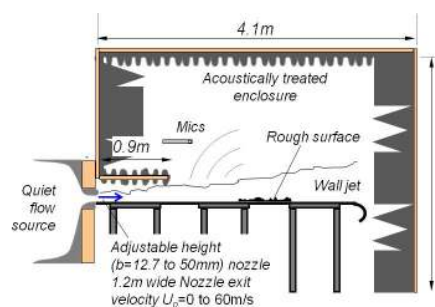


Fig. 4. Illustration of experimental arrangement of the Va Tech group.

geometries that are examined. The physical experiments require facilities that meet three requirements: measurements of boundary layer characteristics (mean and statistical) in order to relate "normalize" sound to TBL properties and to compare with the LES experiments; ability to measure sound in a free field and to define its directivity with respect to the roughness patch; measurement of the wall pressure fluctuations as a expedient metric of the TBL aerodynamic source strength. The experiments are being conducted by 2 complementary groups. The work of Goody *et al* [5] is in n acoustic wind tunnel with the arrangement shown in Fig. 3. This study will focus on larger roughness elements. The open-jet of the wind tunnel is bounded on one side with a rigid wall boundary on which is mounted the various physical roughness panels. Positioned opposite the wall is a directive acoustic array of 63 microphoness that is situated to measure the radiated sound to the near-normal to the plate. A wall-mounted linear microphone array which is situated in the wall plane just downstream of the roughness patch is used to measure the sound emitted in the plane of the wall. These two arrays are used to determine directivity of the sound in two critical directions. Arrays of flush-mounted pin-hole microphones are interspersed among the elements in order to characterize the aerodynamic wall pressure field. Extensive TBL measurements are used to characterize and

support the acoustic measurements; these yield TBL mean wall shear and thicknesses along the streamwise direction. The physical arrangement of Devenport *et al* [6], Fig. 4, was similar although with less focus on measuring far field acoustic directivity and greater focus on measuring the details of wall shear stress and turbulence statistics in the regions near to the roughness elements. This group will address smaller patches and smaller roughness elements. Both Goody *et al* [5] ($\sim$100<$h^+$<$\sim$1900, $h^+$,= $hU_\tau/\nu$,) and Devenport *et al* ($\sim$2<$h^+$<$\sim$82) are modelling random distributions of sand grain roughness as well as the deterministic distributions of hemispherical elements that match the LES experiments.

## 3. Initial measurements and simulations of sound from distributed random roughness elements

The initial exploratory measurements of sound [5,6] were conducted with various roughness sizes and distributions with objectives that included the establishment of the facility limitations. Initial measurements with the rougher [5] wall patches will be discussed here. A most essential step in establishing the physics of the rough-wall TBL sound is to unequivocally measure the sound emitted into the two directions normal and parallel to the wall. Figure 5 discloses results of three test situations. In part (a) of the figure is shown a baseline smooth wall source distribution that is inferred from the array output; part (b) shows the source distribution from 2 rows of roughness elements aligned across the flow direction; part (c) shows the source distribution from a complete patch of approximate dimensions 813 mm (32 in) streamwise by 203 mm (8 in) span. The roughness size for this measurement is in the vicinity of $h^+\sim$1800. These source maps are determined by inversion of the array output [5] and provide maps of mean-square sound pressure per unit resolution area (roughly 50 mm by 50 mm resolution at 2000 Hz and proportional to frequency), with the mean-square sound referred to a reference range. Normalization of the map on the resolution area and then integration over the entire map area yields the overall mean-square sound at that reference range. We see in Figure [5] that the measured sound level increases monotonically as roughness is added to the patch and that the greatest contribution to the sound is from near the leading edge of the patch.

Figure 6 shows additional source maps for a patch of lesser roughness, $h^+$= $\sim$780. Again, flow is from right to left. These maps show similar distributions of sources and also shows dominance by the leading edge elements. Note that the levels are $\sim$5dB lower than for the larger elements.

An analytical simulation was conducted to calculate the sound from a finite roughness area in which the roughness dipoles were given random strength and orientation as well as being reflected by the rigid wall plane. The orientations of the dipoles were simulated to have vector orientations aligned as if they were flow-induced stresses that would occur on the elements of the roughness. These generally orient themselves as shear fluctuations in the direction of the mean flow, but with directions varying slightly element-to-element within some limit. The simulation thus mimicked the experimental arrangement in the size and

orientation of the patch and its instantaneous dipole distribution relative to the array. The overall magnitude of the shear stresses was tapered to matched the observed [10] evolution of wall shear along the patch's streamwise direction. The simulated source map is compared with the measured one in Figure 6. Results suggest that the leading roughness elements in a finite patch of roughness contribute heavily to the overall sound radiated. Figure 7 shows the calculated directivity pattern of the sound as well as superposition of the measured sound levels at 0 and 90 degrees from the flow direction. The directivity pattern was
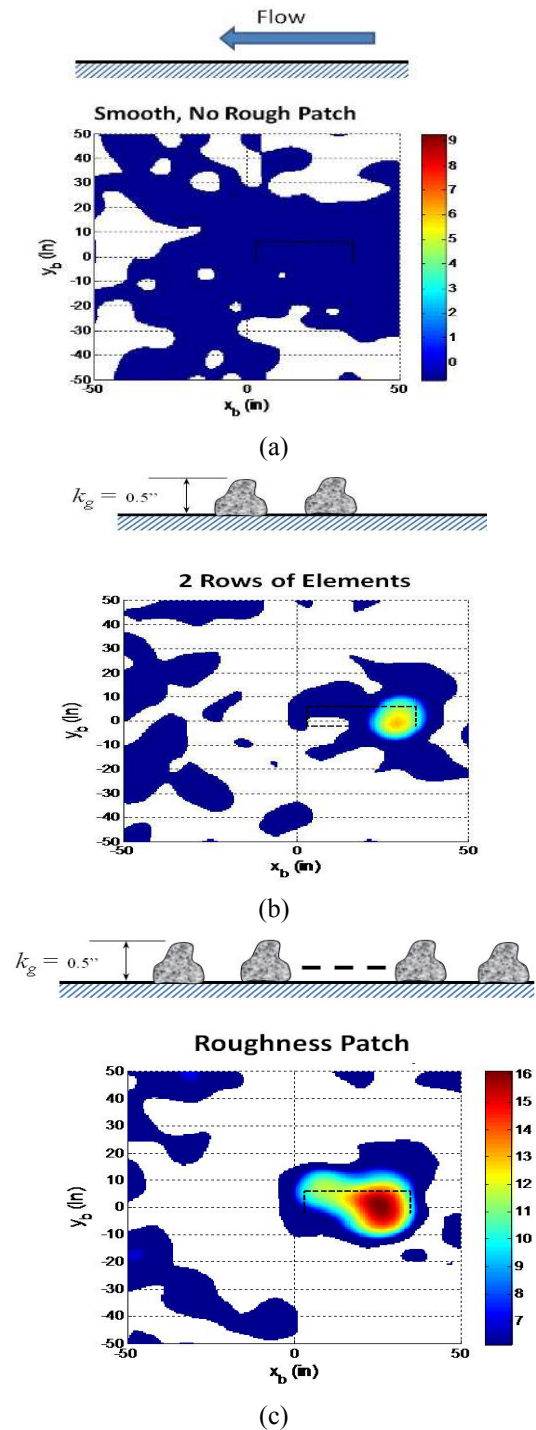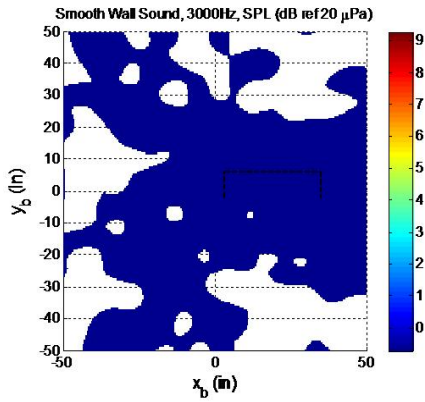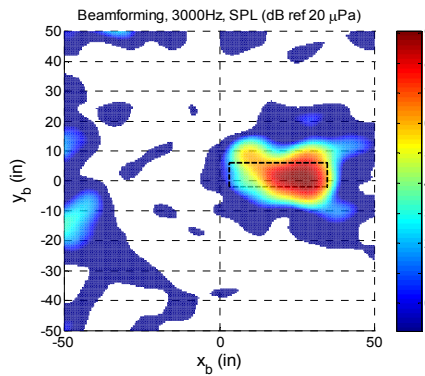


Fig. 5 Images of source distributions on roughness patch at ~42.7 m/s and 3000 Hz. (a) baseline smooth wall, (b) 2 rows of roughness elements, (c) patch of continuous random distribution of elements. The colorbar in part (c) applies to part (b).

plotted by scaling the calculated level on the wall to match the measured value. It would appear that the measurements to this point generally agree with the initial hypothesis of dominance of the sound in the plane of the wall and that the sound from a finite patch of roughness with a developing TBL dominates at its leading edge.



(a)   No Roughness Baseline



(b)   Rough Patch, h = ~5mm.

Fig. 6 Images of source distributions on roughness patch at ~42.7 m/s and 3000 Hz. (a) baseline smooth wall, (b) patch of continuous random distribution of elements, $h^+$~550.
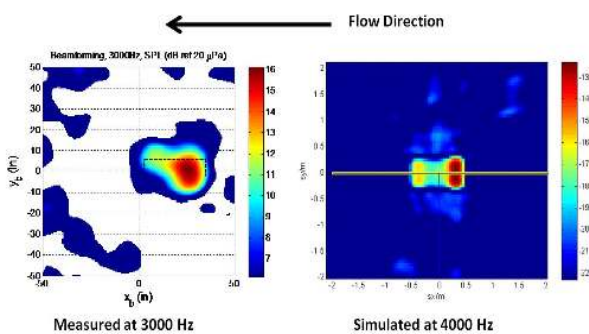


Fig. 7. Measured and calculated images for source distributions of roughness patch  at 3000 to 4000 Hz.
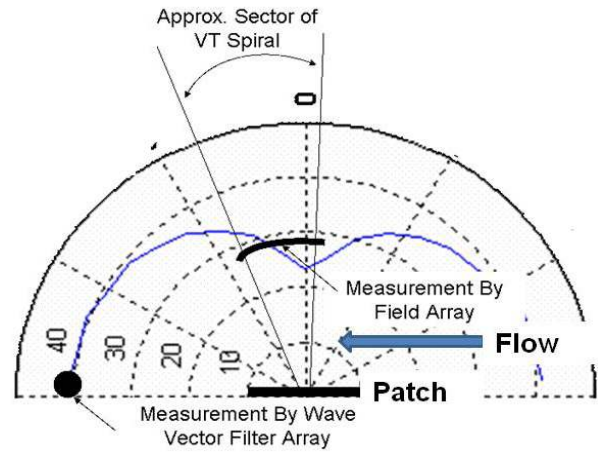


Fig. 8 Directivity pattern of distributed wall roughness at 6000 Hz; points are measured using free field (VT spiral array) and wall-mounted arrays;  line is calculated using the simulation then scaled  to the value obtained by the wave vector filter.

## 4   The relationship between the radiated sound and fluctuating wall pressure

Devenport [6] has examined the relationship between the fluctuating wall pressure and the radiated sound in the free field region above the wall. Figure 8 shows ratios of the measured sound pressure and wall pressure fluctuation spectra for patches of distributed roughness similar to that discussed above, but smaller, i..e. 305 mm streamwise (~20 δ) by 610mm span, with $h^+$ also smaller. It was found that further normalization on the measured geometric size was required to align the measurements into a single group. This normalization arises from a dimensional analysis that of shear stress dipoles that has two alternative forms depending on whether the dipole strength is determined by Rayleigh-like scattering or by aerodynamic drag at the roughness elements. Thus for the drag mechanism, the relationship between the wall pressure and sound pressure involves an $h^2$ and this is reflected in the scaling shown in Figure 8b.

A dimensional analysis of the roughness-generated sound discloses alternative parametric dependences depending on whether the dipoles that are attached to the elements are generated from reactions to Rayleigh-like scattering or to aerodynamic interaction, thus,

$$\Phi_{rad}(\omega) = \left[\overline{F^2(\omega)}\right]\left[\frac{\omega}{r}\frac{\cos\theta}{c_o}\right]^2\left[\frac{A_{surface}}{l_x l_y}\right]G(h^+, \vec{k}_c \bullet \vec{\ell}) \qquad (1)$$

where the bracketed terms represent respectively the spatial average spectrum of forces on the elements, the compact dipole Green function, the statistical number of radiating elements, and a geometry-dependent function that represents dependence on  roughness size, $h^+=hU_\tau/\nu$, and the projection of the mean convection wave number on the roughness spacing vector $\vec{\ell}$. For the sound determined by aerodynamic interstitial flow this becomes
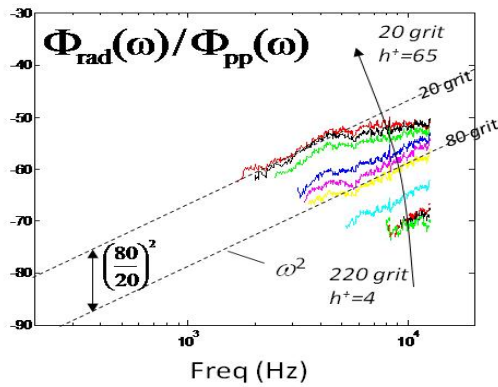
(a) Normalization on surface pressure alone.
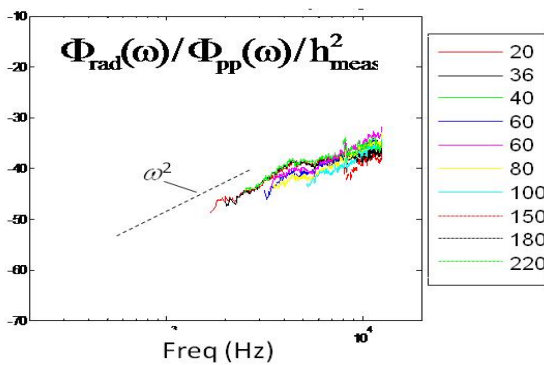


(b) Normalization on surface pressure and roughness measured height.

Fig. 8. Spectrum of radiated sound normalized on wall pressure spectrum.

$$\Phi_{rad}(\omega) = \left[\overline{\Phi_{pp}(\omega)}\right][M]^2 \left[\frac{A_{surface}}{r^2}\right]\left[\frac{\omega h}{U_\infty}\right]^2 \cos^2\theta \cdot G_d(h^+, \vec{k}_c \bullet \vec{\ell}) \quad (2)$$

and for inviscid Rayleigh-like scattering of convected TBL pressure

$$\Phi_{rad}(\omega) = \left[\overline{\Phi_{pp}(\omega)}\right][M]^2 \left[\frac{A_{surface}}{r^2}\right]\left[\frac{\omega h}{U_\infty}\right]^4 \cos^2\theta \cdot G_s(h^+, \vec{k}_c \bullet \vec{\ell}) \quad (3)$$

where M is free stream Mach number, r is range, $U_\infty$ is free stream velocity, $\left|\overline{\Phi_{pp}(\omega)}\right|$ is the area-averaged wall pressure over $A_{surface}$.

# 5    Conclusion

Overall, the data presented here suggests that the parametric equation (2) best defines the radiated sound from rough walls in the fully-rough regime when the roughness elements are evenly and randomly dispersed over the area. Additional on-going work suggests equation (3) best defines sound in the transitional ranges of $h^+$ between hydraulically smooth and fully rough. This is suggested by a slight lack of collapse for the smaller elements in Figure 8b. LES experiments [9] on 1 and 2 element microcosms of a rough wall currently indicate that it is difficult to conclusively separate sound-generation mechanisms, but that a second element in the wake of another is the dominant radiator of the two elements.  Thus the LES

clarifies the importance of viscous interaction between the element and flow.

# Acknowledgments

# References

[1] W.K. Blake, *Mechanisms of Flow Induced Sound and Vibration*, Academic Press, 1986.

[2] Hersh, A.S., 1983, "Surface Roughness Generated Flow Noise, AIAA-83-0786.

[3] Farabee, T. and Geib, E., 1991, "Measurements of Boundary Layer Pressure Fluctuations at Low Wavenumbers on Smooth and Rough Walls," Proceedings of the Int'l. Mech. Eng. Cong. and Expo., NCA Vol. 11, pp. 55-68.

[4] Howe, M.S., 1988, "The Turbulent Boundary-Layer Rough-Wall Pressure Spectrum at Acoustic and Subconvective Wavenumbers," Proceedings of the Royal Society of London A, Vol. 415, pp. 141-161.

[5] Goody, M.C., Anderson, J.A., Stewart, D.O., and Blake, W.B., "Experimental Investigation of sound from flow over a rough surface," Session: NS07/2 – Aeroacoustics, Paris-08, 2008.

[6] Devenport, W., Glegg, S., Alexander, N., Smith,B.," The mechanisms of roughness noise", Session: NS07/1 – Aeroacoustics, Paris-08, 2008.

[7] Martinez, R. Et al, "Understanding Roughness Noise: Progress in Analytical Modelling and Testing, Part 2: Comparison of Calculations to Data" Proceedings of NCAD2008 NoiseCon2008-ASME NCAD July 28-30, 2008, Dearborn, Mi

[8] Martinez, R. et al, "Understanding roughness noise: Progress in analytical modelling and testing, Part 2: Comparison of calculations to data" Proceedings of of NCAD2008 NoiseCon2008-ASME NCAD July 28-30, 2008, Dearborn, Mi

[9] Wang, M. and Yang, Q., "Large-eddy simulation of roughness-generated boundary-layer noise" Session NS07/1-Aeroacoustics, Paris-08, 2008

[10] Yeh, Y.-F. and Nickerson, E.C. "Air flow over roughness discontinuity", Colorado State University Report, CER70-71FFY-ECN6, July 1970.

[11] Grissom,D., Smith,B., Devenport, W., and Glegg,S., "Rough-Wall Boundary layer Noise: An Experimental Investigation" AIAA paper 2007